

In vitro evaluation of multiple arterial stenoses using three-dimensional power Doppler angiography

Zhenyu Guo, PhD, Louis-Gilles Durand, PhD, Louis Allard, MSc, Guy Cloutier, PhD, and Aaron Fenster, PhD, *Washington, D.C.; Montreal, Canada; and London, Ontario, Canada*

Purpose: The study was done to improve quantification of multiple arterial stenoses and to investigate a new imaging technique for lower limb arteries. Three-dimensional power Doppler angiography was used to quantify in vitro arterial stenoses.

Methods: We built two types of artery phantoms containing multiple stenoses. One used stenotic porcine arteries, and the other was designed to control the proximal and distal stenoses while we assessed central stenosis of a wall-less agar lumen. Three-dimensional power Doppler angiograms of the flow lumens were generated at different flow rates under steady and pulsatile flow conditions with a PowerPC 8500 computer-based three-dimensional ultrasound imaging system. This experimental system works off-line, performs three-dimensional acquisition, reconstruction, and display of ultrasound images. Images of flow lumens were compared with the measured B-mode images or the true geometry.

Results: This technique produces good three-dimensional angiographic images of the flow lumen, and multiple stenoses do not affect the diagnosis of arterial stenoses. With this technique, the average errors for estimating 80% and 50% area reduction stenoses were -10% and -4%, respectively.

Conclusions: Three-dimensional power Doppler angiography has the potential to quantitatively grade multisegmental stenoses in lower limbs and generate a map for vasculature surgery planning. (*J Vasc Surg* 1998;27:681-8.)

Color duplex ultrasonography, which combines color Doppler imaging with Doppler spectral analysis, has been extensively used for the quantification of lower limb arterial stenoses.¹⁻³ Because of fre-

quency aliasing and sensitivity to background noise, attempts to use color Doppler imaging to create a reliable anatomic image have not been successful. It is mainly used to position the Doppler sample volume for Doppler spectral analysis to quantify stenoses. The accuracy of color duplex ultrasonography is widely recognized, but the results of some studies indicate that Doppler spectral analysis is less sensitive and accurate for stenosis quantification when there are multisegmental arterial stenoses in lower limbs.^{4,5} This can be attributed to the fact that the Doppler spectral waveform and the maximum velocity measured at one stenosis are modified by the presence of other stenoses in the proximal or the distal arterial segments.

Another ultrasound imaging method, power Doppler imaging, provides angiographic-like images of the flow lumens. Instead of displaying the mean Doppler frequency shift as in color Doppler imaging, power Doppler imaging displays the integrated power of the Doppler signal.⁶ Because the power of the background noise is lower than that of the flow signal, the noise is represented as a homogeneous background color, increasing the dynamic range and

From the Department of Electrical Engineering and Computer Science, The George Washington University, Washington, D.C. (Dr. Guo); Laboratory of Biomedical Engineering, Clinical Research Institute of Montreal, Montreal, Canada (Allard, Drs. Durand and Cloutier); and Imaging Research Laboratories, The John P. Robarts Research Institute, London, Ontario, Canada (Dr. Fenster).

Supported in part by grants from the Medical Research Council of Canada (Dr. Fenster) and the Heart and Stroke Foundation of Quebec (Drs. Durand and Cloutier).

Some parts of this paper were presented in conference papers at the Canadian Conference on Electrical and Computer Engineering, Calgary, Canada, May 1996, and at the Society of Photo-Optical Instrumentation Engineers International Symposium on Medical Imaging, Newport Beach, Calif., February 1997.

Reprint requests: Dr. Zhenyu Guo, Department of Electrical Engineering and Computer Science, The George Washington University, Washington, DC 20052.

Copyright © 1998 by the Society for Vascular Surgery and International Society for Cardiovascular Surgery, North American Chapter.

0741-5214/98/\$5.00 + 0 24/1/87251

substantially increasing the sensitivity to blood flow. Because Doppler power backscattered from blood mainly depends on the number of red blood cells within the Doppler sample volume, power Doppler imaging is nearly independent of Doppler angle and flow velocity,⁷ which assists in perceiving vessel continuity. For these reasons, power Doppler imaging is a useful technique for mapping the arterial lumen, and it can be called power Doppler angiography.

Commercial ultrasound systems can only provide two-dimensional (2D) images, which limits stenosis assessment. In this study, we tried to use power Doppler imaging to create accurate blood vessel cross-sectional images that can then be reconstructed into accurate three-dimensional (3D) power Doppler angiograms, which are used to locate and measure the severity of stenoses. The 3D power Doppler angiography has been used to image the vasculature of the prostate, liver, spleen,⁸ kidney,^{8,9} and placenta.⁹ Because power Doppler angiography directly maps the flow lumen, it should not be affected by the presence of multisegmental arterial stenoses. The purpose of this study was to investigate the evaluation of *in vitro* multiple stenoses with 3D power Doppler angiography.

METHODS

Two types of stenotic artery phantoms were built; one was based on a porcine artery, and the other was based on a wall-less lumen in agar. The porcine artery phantom was used to reflect the almost true clinical situation, and the wall-less lumen phantom was used to reduce the imaging artifact due to wall attenuation. Each arterial phantom was composed of a Plexiglas box containing a tissue mimic composed of a water and agar gel¹⁰ and a stenotic porcine artery or an agar lumen. Glycerol (8%) was added to the tissue mimic to increase its acoustic velocity to that of real tissue, and 3% 50 μ m cellulose ultrasound-scattering particles (S-5504 Sigmacell, Sigma-Aldrich Canada Ltd., Oakville, Ontario, Canada) were added to provide an acoustic attenuation equivalent to that of tissue. For the porcine arterial phantom, sequential stenoses were created by partially tying the artery with nylon tapes, fixing it in formalin for 12 hours, and mounting it in a Plexiglas box with flow connectors. The box was then filled with molten tissue mimic. Two of these porcine artery phantoms were built; one had relatively long stenoses with a nonobstructed mean diameter of 13.8 mm (measured from the 3D B-mode image as discussed later), and another one had relatively short stenoses with a nonobstructed mean diameter of 12.8 mm.

The wall-less agar lumen phantom was built to study the influence of a proximal stenosis, a distal stenosis, and proximal and distal stenoses on a central stenosis with known geometry. The central stenosis was a wall-less agar lumen containing a stenosis of 20 mm long. This center stenosis was formed by pouring the molten tissue mimic around two brass rods jointed at two tapered ends and then removing the two rods from both sides after the tissue mimic set. Each brass rod had a diameter of 7.96 mm, which is similar to that of femoral artery. The tapered ends has a cosine shape as described elsewhere.⁷ Silicone tubes with the same inner diameter as the agar lumen were connected to the central stenosis, and specially designed strangling devices, as described elsewhere,¹¹ were used to form the proximal and distal stenoses with 70% area reduction. For this study, two wall-less agar stenosis models were made; one had an 80% area reduction, and the other had a 50% area reduction. For each wall-less stenosis, the following three adjacent stenosis conditions were created and tested: with a proximal stenosis, with a distal stenosis, and with a proximal and a distal stenosis. The distance between the proximal or the distal stenosis and the central wall-less stenosis was 10 tube diameters (79.6 mm). After the tissue mimic sets, it does not absorb water, and the phantoms were kept in a water bath. Because we used the high-strength agar (A-6924), the formed wall-less lumen had the exact geometry of the brass rod. The shape of the brass rod was equalled the true geometry of the stenosis.

A blood-mimicking fluid composed of a solution of 70% water and 30% glycerol (viscosity of 3.5 cp) was used in this study. Cornstarch was added at 10 g/L to provide ultrasound-scattering particles. A centrifugal pump (Biomedicus 540, Medtronic, Minneapolis, Minn.) connected with a custom-made, computer-controlled pulsatile apparatus was used to circulate the blood mimic through the phantoms in steady and pulsatile flows. The pulsatile apparatus included two rotors that periodically squeezed the circulation rubber tube when pulsatile flow was required. For the porcine artery phantoms, flow rates of 10, 15, 20, 25, and 30 ml/sec (mean flow rate for steady flow and peak flow rate for pulsatile flow) were used. For the wall-less phantoms, flow rates of 5, 7.5, 10, 12.5, and 15 ml/sec were used. In steady flow, these flow rates correspond to flow velocities through the nonobstructed wall-less lumen between 10 and 30 cm/sec.

We used an ATL Ultramark 9 HDI ultrasound system (Advanced Technology Laboratories, Bothell,

Wash.) with a 38 mm aperture linear array probe. The probe was operated at 10 MHz for B-mode imaging and 6 MHz for power Doppler imaging. A gray-scale was selected in this study to map the Doppler power. A color gain of 65% was selected to optimize the 2D power Doppler images visually. The pulse repetition frequency and the wall filter were set to 1500 and 50 Hz, respectively. The persistence level (i.e., number of video frames averaged) was 5, providing a good vessel lumen contour depiction. These imaging parameters were kept unchanged throughout the experiments.

A 3D ultrasound imaging system developed at The John P. Roberts Research Institute¹² and produced by Life Imaging Systems Inc. (London, Canada) was used to perform 3D power Doppler angiography. This system includes a PowerPC 8500 computer and a motor-driven translation assembly to move the ultrasound probe. The linear array probe was mounted on the translation assembly with a Doppler angle of 70 degrees. Water was used to couple the probe to the tissue mimic. For each porcine artery and for each flow rate, 250 contiguous 2D power Doppler images, 0.25 mm apart, were acquired while translating the probe along the artery to scan a distance of 62.5 mm. Every 2D image had the dimensions of 192×250 pixels with the resolution of 8 bits/pixel. Working in zoomed mode of the ultrasound system, the resulting voxel dimensions in the x, y, and z directions were calibrated and found to be $0.123 \text{ mm} \times 0.109 \text{ mm} \times 0.25 \text{ mm}$. For each wall-less stenosis under evaluation, 180 contiguous 2D power Doppler images, also 0.25 mm apart but having the dimensions of 160×200 pixels, were acquired for each combination of the proximal and distal stenoses at every flow rate. The voxel dimensions for the wall-less lumens in the x, y, and z directions were $0.084 \text{ mm} \times 0.076 \text{ mm} \times 0.25 \text{ mm}$. The time to acquire these 2D images was less than 1 minute. Because power Doppler imaging is nearly flow velocity independent and a high persistence was used, the power Doppler image was relatively constant, and flow gating was not used when the flow was pulsatile.

The 3D reconstruction was performed on each set of 2D images by shearing to compensate the Doppler angle to generate a 3D volume using the same computer. A texture mapping technique was used to display the 3D power Doppler angiograms.

For each porcine artery, a 3D B-mode image was generated with a zero flow rate. Successive cross-sectional areas of the flow lumen for each artery were measured on the 3D B-mode image by planimetry with facilities of the 3D display software at an incre-

ment of 2 mm along the artery. These measurements were repeated four times for each 3D B-mode image. For each 3D power Doppler volume, the cross-sectional flow area was computed at every 2D slice (0.25 mm apart) perpendicular to the arterial axis by counting the pixels corresponding to the flow field with a threshold of 25% of the maximum value of the power map to separate the flow field from background noise. This analysis was performed for every flow rate under steady and pulsatile flow conditions. Mean flow areas were calculated by averaging the flow areas of all the flow rates tested. The measured mean cross-sectional flow areas from 3D power Doppler angiograms were plotted with those from 3D B-mode images.

Because the true geometry of the wall-less stenoses were known (i.e., geometry of the brass rods), their true cross-sectional areas were used as references. At each proximal and distal stenosis condition, the cross-sectional flow areas of the wall-less stenosis were calculated by pixel counting for each flow rate. The mean flow areas calculated as described previously were plotted along the lumen axis with the true areas for comparison. We also measured the cross-sectional flow areas of the wall-less stenoses and the areas of prestenotic lumen by planimetry. The percentage of area reduction was computed as the ratio of the minimum flow area at the stenosis to the maximum prestenotic flow area. For each proximal and distal stenosis combination, the mean percent of area reduction was computed by averaging the results of all the flow rates.

RESULTS

Figs. 1 and 2 show the 3D B-mode images and power Doppler angiograms of the porcine arteries with short and long multiple stenoses generated with a steady flow of 25 ml/sec. Visual inspection of all B-mode images and power Doppler angiograms obtained for the different flow rates tested strongly suggests that performance of 3D power Doppler angiography is not affected by the presence of multiple stenoses. The low power in the two stenoses in Fig. 1B resulted from the acoustic shadowing produced by the nylon tapes used to create the stenoses; we neglected to remove them before pouring the tissue mimic. Because the nylon tapes used to create stenoses used for Fig. 2 were removed after fixing the artery in formalin and before pouring the tissue mimic, there is no power attenuation in the two stenoses in Fig. 2B.

Fig. 3 shows the 3D power Doppler angiograms of the 80% and 50% stenotic wall-less lumens gener-

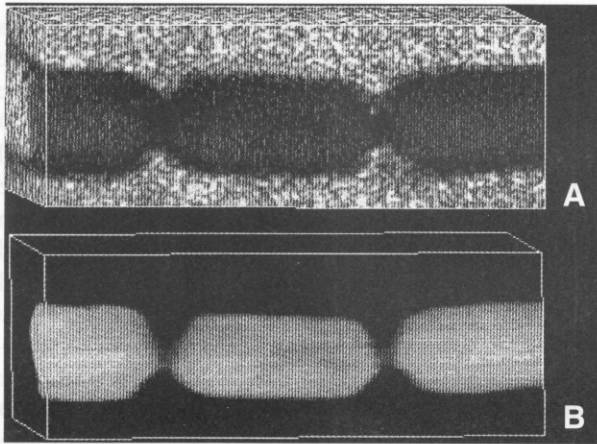


Fig. 1. Three-dimensional (3D) B-mode image (A) and 3D power Doppler angiogram (B) of the porcine artery with short stenoses. A steady flow of 25 ml/sec was used to generate the 3D power Doppler angiogram.

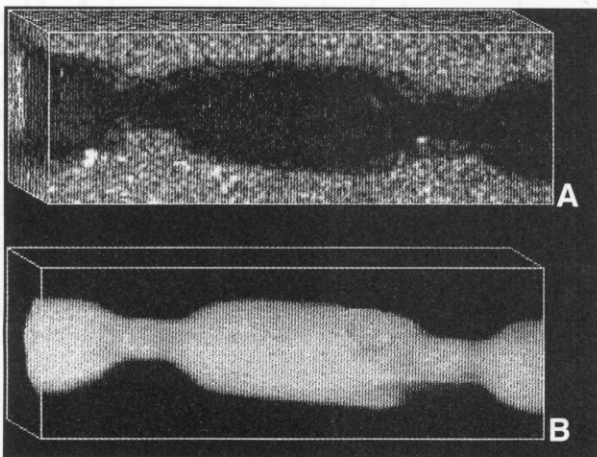


Fig. 2. Three-dimensional (3D) B-mode image (A) and 3D power Doppler angiogram (B) of the porcine artery with long stenoses. A steady flow of 25 ml/sec was used to generate the 3D power Doppler angiogram.

ated with a pulsatile flow having a peak flow rate of 15 ml/sec. The power Doppler angiograms are not sensitive to the flow variation, because no flow gating was used to acquire the 2D images that were used to form these 3D angiograms. Fig. 4 shows the 3D power Doppler angiograms of the central 80% stenosis generated with a steady flow of 10 ml/sec for different conditions of proximal and distal stenoses. In Fig. 4A through 4D, no difference can be observed in the appearance of the central stenosis.

Fig. 5 plots the mean cross-sectional flow area against a length of the porcine artery with multiple stenoses. The top, solid curve represents the cross-

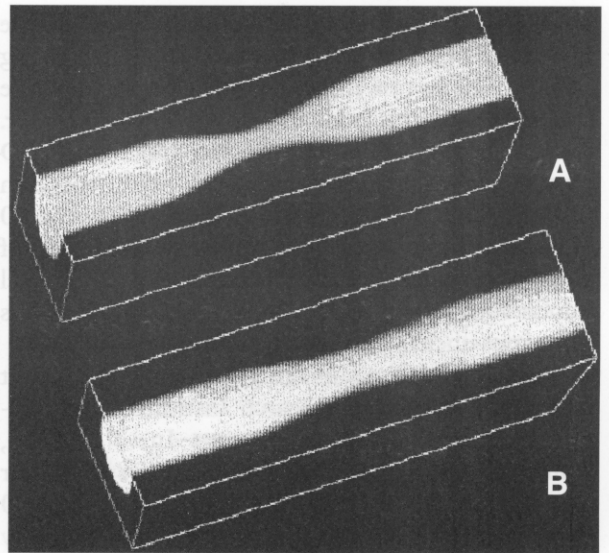


Fig. 3. Three dimensional (3D) power Doppler angiograms of the wall-less agar lumen show an 80% area reduction stenosis (A) and a 50% area reduction stenosis (B). Pulsatile flow with a peak flow rate of 15 ml/sec was used to generate these two 3D angiograms.

sectional flow areas measured from 3D power Doppler angiograms, and the open circles, with error bars for one standard deviation, represent those from 3D B-mode images. The bottom curve of each panel corresponds to one standard deviation of the mean areas measured from 3D power Doppler angiograms. Fig. 5A corresponds to the short stenoses and Fig. 5B to the long stenoses. These results are for steady flow, but the pulsatile flow experiments provided almost identical results. The cross-sectional flow areas obtained from 3D power Doppler angiograms (top, solid curve) are in good agreement with those obtained from 3D B-mode images (open circles).

Fig. 6 was obtained with pulsatile flow condition and shows the measured mean cross-sectional flow areas (top, solid curve) from 3D power Doppler angiograms of the 80% stenotic wall-less lumen, with the true areas plotted as dashed curves. The solid curve at the bottom of each panel represents one standard deviation of the mean area. The panels correspond to the conditions of no proximal and distal stenosis (Fig. 6A), one proximal stenosis (Fig. 6B), one distal stenosis (Fig. 6C), and one proximal and one distal stenosis (Fig. 6D). No difference can be seen from Fig. 6A through 6D, indicating that the presence of multiple stenoses does not seem to affect the performance of 3D power Doppler angiography. From the solid curves at the bottom of the panels, it

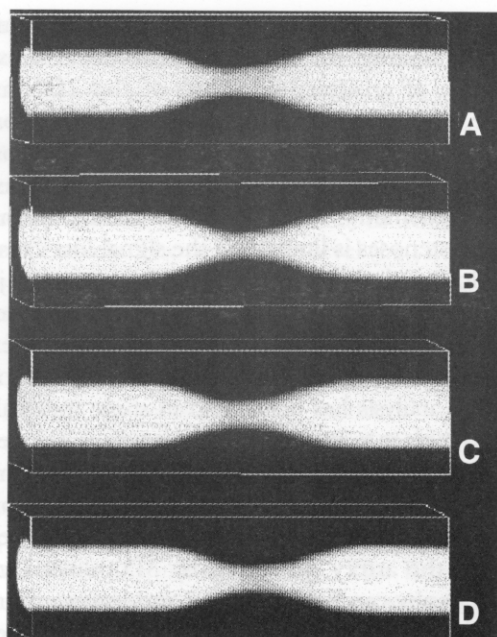


Fig. 4. Three-dimensional power Doppler angiograms of the central stenosis with an 80% area reduction generated with a steady flow of 10 ml/sec. **A**, Without proximal and distal stenoses. **B**, With a 70% proximal stenosis. **C**, With a 70% distal stenosis. **D**, With proximal and distal stenoses of 70%.

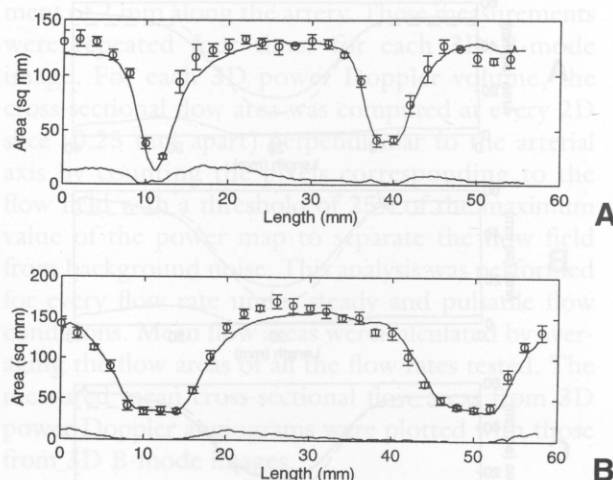


Fig. 5. Cross-sectional flow areas are plotted against the length of the porcine artery for short multiple stenoses (**A**) and long multiple stenoses (**B**). The *top, solid curve* represents the mean area obtained by averaging five 3D power Doppler angiograms generated for five steady flows with flow rates of 10, 15, 20, 25, and 30 ml/sec. The *bottom, solid curve* corresponds to one standard deviation of these means. Cross-sectional areas estimated from 3D B-mode images are shown as *open circles*, and the *error bars* represent one standard deviation.

Table I. Measured cross-sectional area reduction of wall-less agar stenotic lumens for steady and pulsatile flow.

| | Area reduction (%) | | | |
|-----|--------------------|----------------|--------------|----------------|
| | 80% Stenosis | | 50% Stenosis | |
| | Steady flow | Pulsatile flow | Steady flow | Pulsatile flow |
| NO | 68.8 ± 3.7 | 70.0 ± 3.0 | 45.6 ± 1.2 | 45.0 ± 2.5 |
| P | 70.6 ± 2.1 | 70.8 ± 2.3 | 47.4 ± 2.1 | 47.6 ± 1.2 |
| D | 69.0 ± 2.3 | 69.8 ± 2.3 | 46.4 ± 1.5 | 46.0 ± 1.6 |
| P+D | 70.0 ± 1.9 | 70.4 ± 3.4 | 47.6 ± 2.8 | 46.8 ± 0.8 |

NO, Without proximal and distal stenoses; P, with a proximal stenosis of 70% area reduction; D, with a distal stenosis of 70% area reduction; P+D, with proximal and distal stenoses of 70% area reduction.

can be seen that the values of standard deviation are larger in the zones proximal and distal to the stenosis; this results from the wall filter that removed the Doppler power of low flow velocities in these zones. Although not shown here, the pulsatile flow experiments demonstrated similar results.

Table I shows the measured flow area reduction for wall-less agar stenotic lumens at different flow conditions and for different combinations of proximal and distal stenoses. The presence of multiple stenoses does not affect stenoses quantification by

using 3D power Doppler angiography. Steady and pulsatile flow conditions provide almost identical results; on average, the 80% stenosis was measured as a 70% stenosis (−10% area reduction error), and the 50% stenosis was quantified as a 46% stenosis (−4% area reduction error).

DISCUSSION

For patients with symptoms and signs of lower limb arterial occlusive disease, segmental blood pressure measurements provide a rough estimate of the

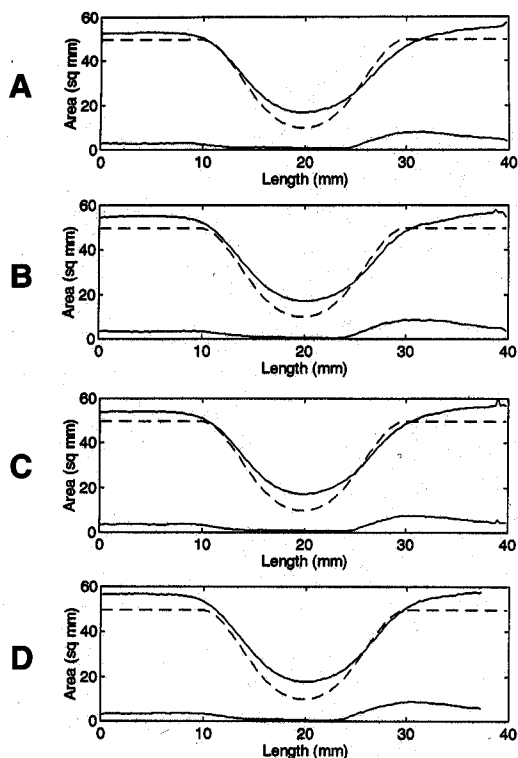


Fig. 6. The cross-sectional flow area is plotted against the length of the 80% area reduction stenotic wall-less lumen. The areas are means averaged from five 3D power Doppler angiograms generated with the use of pulsatile flow with flow rates of 5, 7.5, 10, 12.5, and 15 ml/sec. The *bottom, solid curve* corresponds to one standard deviation of the means. The true cross-sectional flow areas are shown as the *dashed curve*. **A,** Without proximal and distal stenosis. **B,** With a 70% proximal stenosis. **C,** With a 70% distal stenosis. **D,** With proximal and distal stenoses of 70%.

severity of the disease and the occlusion locations. This information is used to divide patients into two groups on the basis of "inflow," or iliac disease, and "outflow," or femoropopliteal disease.¹³ However, pressure measurement does not accurately quantify the severity of stenoses and does not provide the length of diseased segment and the anatomic location of the disease. This information is essential for designing limb-salvaging operations, because the therapeutic options available to patients with symptomatic lower limb arterial occlusive disease depend on the underlying anatomy.

Conventional contrast angiography has provided the anatomic information necessary to plan vascular interventional therapy. However, this technique is invasive, requiring injection of iodinated contrast and exposing the patients to radiation risks. Multiple

occlusions can block the distribution of contrast, thereby failing to opacity patent distal vessels.¹⁴ Because of arbitrary selection of the 2D imaging plane, quantification of stenoses using contrast angiography may be inaccurate. Magnetic resonance angiography can produce 3D images of vascular lumen geometry,¹⁵ but its performance in imaging arterial stenoses is limited by the signal loss caused by the flow turbulence encountered in stenotic jets,¹⁶ leading to an apparent interruption of the vessel and erroneous quantification of the true diameter and length of the occlusive lesion. Although Doppler spectral analysis has been used in some medical centers to replace x-ray angiography to diagnose stenoses and to plan surgery, the presence of multisegmental stenoses decreases the diagnostic power of the Doppler spectral analysis. A 3D morphologic description of the artery generated by 3D power Doppler angiography can help surgeons and interventionalists to delineate diseased vessels for bypass procedures and to identify stenoses amenable to angioplasty.

By using the velocity ratio as a discriminant feature, Allard et al.¹¹ demonstrated that a shorter distance between a proximal or a distal stenosis and the stenosis being assessed has more effect on the diagnostic accuracy than a longer distance. With a distance between stenoses of only 10 vessel diameters, we found that multiple stenoses did not affect the diagnostic accuracy of 3D power Doppler angiography. For clinical multisegmental stenoses, the diagnostic performance of 3D power Doppler angiography should not be affected by the presence of stenoses at different arterial segments.

The flow areas measured by power Doppler were generally larger than the true lumen areas (Fig. 6), probably because of the finite sample volume of the ultrasound system. When the sample volume is located at the vessel boundary, with part within the flow field and part outside of the flow field, the region occupied by the sample volume is mapped as a flow field on the power Doppler image, enlarging the apparent flow lumen. However, the Doppler power from this sample volume is lower than the one from a sample volume within the lumen because of a lower number of scattering particles and the wall filter effect. In Fig. 7, we plotted the backscattered Doppler power across the diameter of the imaged lumen. A clear power transition at the edge of the flow boundary can be seen. The selection of the threshold used to separate the flow field from the background can affect the estimation of the flow area, as in digital subtraction angiography.

One design requirement of a lower limb arterial

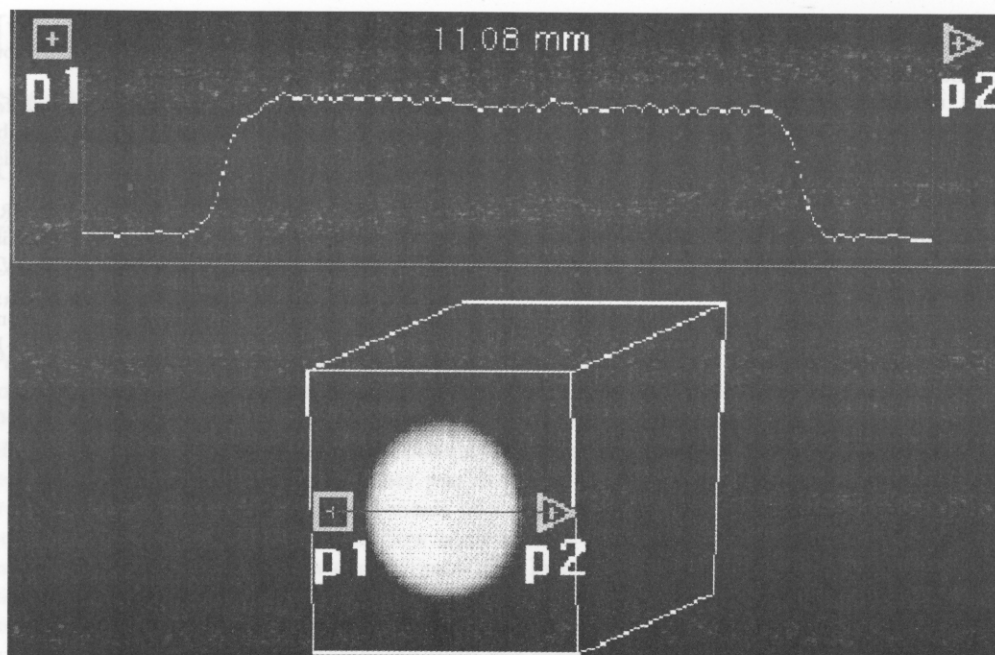


Fig. 7. Three-dimensional power Doppler angiogram with a cross-sectional cutting plane provides a transverse view of the flow lumen. The *upper curve* represents the Doppler power plotted across the diameter of the lumen.

imaging system is the necessity to image the entire arterial tree. Linear probes such as the one used in this study provide sufficient resolution, but the field of view of the linear probe is normally small (<4 cm). Our scanning system can be modified to scan in a raster pattern to form a large field of view. Another requirement of lower limb artery imaging system is that the technique used must be sensitive to slow flow, such that flow in reconstituted distal runoff vessels and in aneurysmal vessel segments can be thoroughly visualized. Originally designed to map the slow flow, power Doppler angiography can meet this requirement.

This *in vitro* study provides promising results for quantifying lower limb arterial stenoses using 3D power Doppler angiography. To extend this technique to clinical practice, further investigations are required. As the results indicate, power Doppler imaging is not sensitive to flow variation, but the image disappears when the flow velocity is below the cut-off velocity set by the clutter cancel wall filter. For lower limb application, the power Doppler image is pulsatile because there is significant reverse flow in the arteries of the lower limb during diastole, indicating that the flow velocity can sometimes go below the cut-off velocity. Flow-gating image acquisition should be used in clinical application. Studies

comparing 3D power Doppler angiography with 2D power Doppler imaging and contrast angiography for the quantification of multiple stenoses are needed to validate 3D power Doppler angiography before it can be used in clinical practice.

REFERENCES

1. Leng GC, Whyman MR, Donnan PT, Ruckley CV, Gillespie I, Fowkes GR, Allan PL. Accuracy and reproducibility of duplex ultrasonography in grading femoropopliteal stenoses. *J Vasc Surg* 1993;17:510-7.
2. Moneta GL, Yeager RA, Antonovic R, Hall LD, Caster JD, Cummings CA, Porter JM. Accuracy of lower extremity arterial duplex mapping. *J Vasc Surg* 1992;15:275-84.
3. Mulligan SA, Matsuda T, Lanzer P, Gross GM, Routh WD, Keller FS, et al. Peripheral arterial occlusive disease: Prospective comparison of MR angiography and color Duplex US with conventional angiography. *Radiology* 1991;178:695-700.
4. Allard L, Cloutier G, Durand LG, Roederer GO, Langlois YE. Limitations of ultrasonic duplex scanning for diagnosing lower limb arterial stenoses in presence of adjacent segment disease. *J Vasc Surg* 1994;19:650-7.
5. Sacks D, Robinson ML, Marinelli DL, Perlmutter GS. Peripheral arterial Doppler ultrasonography: diagnostic criteria. *J Ultrasound Med* 1992;11:95-103.
6. Rubin JM, Adler RS. Power Doppler expands standard color capability. *Diagn Imaging* 1993;12:66-9.
7. Guo Z, Fenster A. Three-dimensional power Doppler imaging: a phantom study to quantify vessels stenosis. *Ultrasound Med Biol* 1996;22:1059-69.

8. Downey DB, Fenster A. Vascular imaging with a three-dimensional power Doppler system. *AJR* 1995;165:665-8.
9. Ritchie CJ, Edwards WS, Mark LA, Cyr DR, Kim Y. Three-dimensional ultrasonic angiography using power-mode Doppler. *Ultrasound Med Biol* 1996;22:277-86.
10. Rickey DW, Picot PA, Fenster A. A wall-less vessel phantom for Doppler ultrasound studies. *Ultrasound Med Biol* 1995;21:1163-76.
11. Allard L, Cloutier G, Durand LG. Doppler velocity ratio measurements evaluated in a phantom model of multiple arterial disease. *Ultrasound Med Biol* 1995; 21:471-80.
12. Picot PA, Rickey DW, Mitchell R, Rankin RN, Fenster A. Three-dimensional colour Doppler imaging. *Ultrasound Med Biol* 1993;19:95-104.
13. Yucel EK. Magnetic resonance angiography of the lower extremity and renal arteries. *Semin Ultrasound CT MR* 1992;13:291-302.
14. Owen RS, Carpenter JP, Baum RAF, Perloff LJ, Cope C. Magnetic resonance imaging of angiographically occult runoff vessels in peripheral arterial occlusive disease. *N Engl J Med* 1992;326:1577-81.
15. Blatter DD, Parker DL, Ahn SS. Cerebral MR angiography with multiple overlapping thin slab acquisition: Part I. Quantitative analysis of vessel visibility. *Radiology* 1991;179:805-11.
16. Edelman RR. Basic principles of magnetic resonance angiography. *Cardiovasc Intervent Radiol* 1992;15:3-13.

Submitted July 8, 1997; accepted Oct. 30, 1997.